A NONSINGULAR INTEGRAL FORMULATION FOR THE HELMHOLTZ EIGENPROBLEMS OF A CIRCULAR DOMAIN

Jeng-Tzong Chen*, Shyh-Rong Kuo and Kwe-Hoo Chen
Department of Harbor and River Engineering
Taiwan Ocean University
Keelung 202, Taiwan

Key Words: imaginary-part dual BEM; spurious eigenvalues and eigenmodes; Bessel function and Helmholtz equation

ABSTRACT

A nonsingular integral formulation for the Helmholtz eigenproblem is developed in this paper. This novel method contains only imaginary-part kernels instead of complex-part kernels in the complex-valued BEM. Based on the imaginary-part formulation without singular source, no singular or hypersingular integrals are present. Although this formulation avoids the computation of singular and hypersingular integrals, this approach results in spurious eigensolutions. After comparing the results from the dual formulation, the true and spurious solutions can be separated. An analytical example for the eigensolutions of a two-dimensional circular domain is studied. The continuous system can be transformed to a discrete system with circulants. Based on the spectral properties of circulants, the true and spurious solutions for the eigenvalues, boundary modes, interior modes and multiplicities are all examined. The possible failure of Hutchinson's sorting technique of looking at modal shapes is also discussed.

I. INTRODUCTION

Eigenvalues and eigenmodes are often encountered not only in vibration problems, but also in acoustic problems. For the Helmholtz eigenproblems, it is well known that the complex-valued boundary element method (BEM) can determine the eigensolutions by using direct determinant searching (De Mey, 1976). Nevertheless, complex-valued computation is time consuming and not simple. Tai and Shaw (1974) solved the Helmholtz eigenproblem using real-part formulation. Also, a simplified method using only real-part kernel was presented by De Mey (1977). Since only the first eigenvalue was studied, the spurious solutions were not discovered. Also, Hut-chinson replaced the complex-valued kernel with a real-part one to solve plate and membrane vibration problems (Hutchinson, 1985, 1988, 1991). He found the spurious solutions and suggested an easy and practical method to sort out spurious modes by looking at the modal shapes. But whether the technique may fail or not was not discussed. Kamiya *et al.* (1996) also found that MRM is no more than the real part of complex-valued BEM. The method, using only the real-part BEM, was found to be equivalent to the multiple reciprocity method (MRM) if the zeroth-order fundamental solution for MRM is correctly chosen (Yeih *et al.*; 1997, Chen 1999). Both the real-part BEM and MRM result in spurious eigensolutions for one-dimensional rods (Chen and

*Correspondence addressee

Wong, 1997), beams (Yeih *et al.*, 1999) and two dimensional cavities (Chen and Wong, 1999). Numerical experiments using the real kernels were performed for two-dimensional cases with a degenerate boundary (Liou *et al.*, 1999). The relations among the conventional MRM, the complete MRM, the real-part BEM and the complex-valued BEM were discussed by Chen (1999). One advantage of using only the real-part kernels is that real-valued computation is employed instead of complex-valued computation as used in the complex-valued BEM. Another benefit is that tedious derivation as required for the MRM can be avoided. However, three drawbacks of the real formulation have been found to be the occurrence of spurious eigenvalues (Chen and Wong, 1997, 1998; Liou *et al.*, 1999), singular and hypersingular integrals, and failure when it is applied to problems with a degenerate boundary (Chen and Wong, 1998; Chen and Hong, 1999). To deal with the first and third problems at the same time, the framework of the real-part "dual" BEM was constructed to filter out spurious eigenvalues and to avoid nonunique solutions for problems with a degenerate boundary. As for the second problem, to avoid singular and hypersingular integrals, the indirect formulation with fictitious boundary is one approach. To find another alternative method to avoid the singularity problem without using fictitious boundary is the main motivation of this paper. This results in regular formulation with no-source auxilliary system. Solving the eigenproblem in imaginary-part formulation without singularity was the goal of this study.

In this paper, we employ the imaginary-part dual BEM to solve the acoustic problems of a circular domain. This nonsingular formulation results in spurious solutions. After assembling the dual equations for the circular boundary problem, the true and spurious eigenvalues and eigenmodes can be exactly predicted by using the analytical properties of circulants. Also, the true and spurious solutions for boundary modes and multiplicities are both examined. In addition, Hutchinson's sorting technique for true and spurious solutions by looking at modal shapes is addressed.

II. IMAGINARY-PART DUAL INTEGRAL FORMULATION FOR A TWO-DIMENSIONAL ACOUSTIC CAVITY

The governing equation for an acoustic cavity is the Helmholtz equation:

$$(\nabla^2+k^2)\{u(\boldsymbol{x})\}=0,\ \boldsymbol{x}\in D,$$

where ∇^2 is the Laplacian operator, D is the domain of the cavity and k is the wave number, which is the angular frequency over the speed of sound. The boundary conditions considered here are either of the Neumann or Dirichlet type.

Based on the complex-valued dual BEM (Chen and Chen, 1998, Chen *et al.*, 1999a, 1999c), the dual boundary integral equations for smooth boundary points are

$$\pi u(x)=C.P.V.\int_B T_c(s,x)u(s)dB(s) - R.P.V.\int_B U_c(s,x)t(s)dB(s),\ x\in B, \tag{1}$$

$$\pi t(x)=H.P.V.\int_B M_c(s,x)u(s)dB(s) - C.P.V.\int_B L_c(s,x)t(s)dB(s),\ x\in B, \tag{2}$$

where *C.P.V.*, *R.P.V.* and *H.P.V.* denote the Cauchy principal value, the Riemann principal value and Hadamard principal value, respectively; $t(s)=\frac{\partial u(s)}{\partial n_s}$; B denotes the boundary enclosing D. The four kernels in the complex-valued formulation for the two-dimensional Helmholtz problem can be expressed as

$$U_c(s,x)=\frac{-i\pi H_0^{(1)}(kr)}{2}, \tag{3}$$

$$T_c(s,x)=\frac{-k\pi i}{2}H_1^{(1)}(kr)\frac{y_i n_i}{r}, \tag{4}$$

$$L_c(s,x)=\frac{k\pi i}{2}H_1^{(1)}(kr)\frac{y_i \overline{n}_i}{r}, \tag{5}$$

$$M_c(s,x)=\frac{-k\pi i}{2}\{-k\frac{H_2^{(1)}(kr)}{r^2}y_i y_j n_i \overline{n}_j+\frac{H_1^{(1)}(kr)}{r}n_i \overline{n}_i\}, \tag{6}$$

where $H_n^{(1)}(kr)$ denotes the nth order of the first-kind Hankel function; r is the distance between the source point, s, and the field point x; n_i is the ith component of the outnormal vector at s; $\overline{n}_i$ is the ith component of the outnormal vector at x; and $y_i \equiv s_i - x_i$. Although the real-part kernel formulation can solve the problem in the real domain, both singular and hypersingular integrals are encountered (Chen *et al.*, 1999b). Replacing the complex fundamental solutions with imaginary-part kernels, we can avoid the problems of singularity. Therefore, we have

$$U_I(s,x)=Imag\{U_c(s,x)\}=\frac{-\pi J_0(kr)}{2}, \tag{7}$$

Table 1. Properties of the imaginary-part kernels in the dual formulation.

Kernal function $K(s,x)$	$U_I(s,x)$	$T_I(s,x)$	$L_I(s,x)$	$M_I(s,x)$
regularity 2D	$O(1)$	$O(r)$	$O(r)$	$O(r^2)$
Density function $\mu(s)$	$-t$	u	$-t$	u

where $U_I(s,x)=\dfrac{-\pi J_0(kr)}{2}$ for the Helmholtz equation.

$$T_I(s,x)=Imag\{T_c(s,x)\}=\frac{-k\pi}{2}J_1(kr)\frac{y_i n_i}{r}, \tag{8}$$

$$L_I(s,x)=Imag\{L_c(s,x)\}=\frac{k\pi}{2}J_1(kr)\frac{y_i \overline{n}_i}{r}, \tag{9}$$

$$M_I(s,x)=Imag\{M_c(s,x)\}=\frac{k\pi}{2}\{-k\frac{J_2(kr)}{r^2}y_i y_j n_i \overline{n}_j - \frac{J_1(kr)}{r}n_i \overline{n}_i\}, \tag{10}$$

where $J_n(kr)$ denotes the nth order Bessel function of the first kind, and *Imag* denotes the imaginary part. Eqs. (1) and (2) are reduced to

$$0=\int_B T_I(s,x)u(s)dB(s)-\int_B U_I(s,x)t(s)dB(s), \quad x\in B, \tag{11}$$

$$0=\int_B M_I(s,x)u(s)dB(s)-\int_B L_I(s,x)t(s)dB(s), \quad x\in B, \tag{12}$$

where the complex kernels have been replaced by imaginary-part kernels. No free terms are present in Eqs. (11) and (12). Also, all the integrals are nonsingular since there is no singularity in the imaginary-part auxilliary system. The properties are shown in Table 1 which are different from those of the real-part kernels in Table 2. By employing the constant element scheme, Eqs. (11) and (12) can be discretized into the following linear algebraic equations:

$$\{T_I(k)]\{u\}=[U_I(k)]\{u\}, \tag{13}$$

$$\{M_I(k)]\{u\}=[L_I(k)]\{u\}, \tag{14}$$

where the subscript "I" denotes imaginary part, and $[U_I(k)]$, $[T_I(k)]$, $[L_I(k)]$ and $[M_I(k)]$ are the influence matrices with the following elements

$$U_I^{ij}=\int_{B_j} U_I(s_j,x_i)dB(s_j) \tag{15}$$

Table 2. Properties of the real-part kernels in the dual formulation.

Kernal function $K(s,x)$	$U_R(s,x)$	$T_R(s,x)$	$L_R(s,x)$	$M_R(s,x)$
Singularity 2D	$O(ln(r))$	$O(1/r)$	$O(1/r)$	$O(1/r^2)$
Density function $\mu(s)$	$-t$	u	$-t$	u

where $U_R(s,x)=\dfrac{\pi Y_0(kr)}{2}$ for the Helmholtz equation.

$$T_I^{ij}=\int_{B_j} T_I(s_j,x_i)dB(s_j) \tag{16}$$

$$L_I^{ij}=\int_{B_j} U_I(s_j,x_i)dB(s_j) \tag{17}$$

$$M_I^{ij}=\int_{B_j} M_I(s_j,x_i)dB(s_j) \tag{18}$$

where x_i denotes the ith collocation point, s_j is the jth integration element. No singular or hypersingular integrals in Eqs. (15)~(18) can be found.

III. DUAL SERIES REPRESENTATION FOR THE FOUR KERNELS

The four kernels in the dual formulation can be represented by degenerate kernels using the dual series model (Chen, 1998) as follows:

$$U_I(s,x)=Imag\{\frac{-i\pi H_0^{(1)}(kr)}{2}\}$$

$$=\begin{cases} U^i(s,x)=-\sum_{m=-\infty}^{\infty}\frac{\pi}{2}J_m(k\rho)J_m(kR)\cos(m(\theta-\phi)), & R>\rho \\ U^e(s,x)=-\sum_{m=-\infty}^{\infty}\frac{\pi}{2}J_m(kR)J_m(k\rho)\cos(m(\theta-\phi)), & \rho>R \end{cases} \tag{19}$$

$$T_I(s,x)=Imag\{\frac{-i\pi\partial H_0^{(1)}(kr)}{2\partial R}\}$$

$$=\begin{cases} T^i(s,x)=-\sum_{m=-\infty}^{\infty}\frac{\pi k}{2}J_m(k\rho)J'_m(kR)\cos(m(\theta-\phi)), & R>\rho \\ T^e(s,x)=-\sum_{m=-\infty}^{\infty}\frac{\pi k}{2}J'_m(kR)J_m(k\rho)\cos(m(\theta-\phi)), & \rho>R \end{cases} \tag{20}$$

$$L_I(s,x) = Imag\{\frac{-i\pi}{2}\frac{\partial H_0^{(1)}(kr)}{\partial \rho}\}$$

$$= \begin{cases} L^i(s,x) = -\sum_{m=-\infty}^{\infty} \frac{\pi k}{2} J'_m(k\rho) J_m(kR)\cos(m(\theta-\phi)), & R>\rho \\ L^e(s,x) = -\sum_{m=-\infty}^{\infty} \frac{\pi k}{2} J_m(kR) J'_m(k\rho)\cos(m(\theta-\phi)), & \rho>R \end{cases} \quad (21)$$

$$M_I(s,x) = Imag\{\frac{-i\pi}{2}\frac{\partial^2 H_0^{(1)}(kr)}{\partial\rho\partial R}\}$$

$$= \begin{cases} M^i(s,x) = -\sum_{m=-\infty}^{\infty} \frac{\pi k^2}{2} J'_m(k\rho) J'_m(kR)\cos(m(\theta-\phi)), & R>\rho \\ M^e(s,x) = -\sum_{m=-\infty}^{\infty} \frac{\pi k^2}{2} J'_m(kR) J'_m(k\rho)\cos(m(\theta-\phi)), & \rho>R \end{cases} \quad (22)$$

where $x=(\rho, \phi)$, $s=(R, \theta)$, ρ, R, θ and ϕ are defined in Fig. 1. It is found that the kernels for interior ($R<\rho$) and exterior ($R>\rho$) domains are equal and all the potentials across the boundary are continuous.

IV. ANALYTICAL STUDY OF TRUE AND SPURIOUS EIGENVALUES USING THE IMAGINARY-PART DUAL BEM FOR A CIRCULAR BOUNDARY

As mentioned earlier, spurious eigenvalues occur in the real-part or MRM formulations (Chen and Wong, 1997, 1998, Chen *et al.*, 1999b). What happens for the imaginary-part BEM? Here, we will derive the analytical solution for the true and spurious eigeneigenvalues of a circular domain by using the dual series representation model.

If the direct method is employed for a circular problem, the four imaginary-part kernels can be simplified into

$$U_I(s,x) = U(\theta,\phi) = -\sum_{m=-\infty}^{\infty} \frac{\pi}{2} J_m(k\rho) J_m(k\rho)\cos(m(\theta-\phi)) \quad (23)$$

$$T_I(s,x) = T(\theta,\phi) = -\sum_{m=-\infty}^{\infty} \frac{\pi k}{2} J'_m(k\rho) J_m(k\rho)\cos(m(\theta-\phi)) \quad (24)$$

$$L_I(s,x) = L(\theta,\phi) = -\sum_{m=-\infty}^{\infty} \frac{\pi k}{2} J_m(k\rho) J'_m(k\rho)\cos(m(\theta-\phi)) \quad (25)$$

$$M_I(s,x) = M(\theta,\phi) = -\sum_{m=-\infty}^{\infty} \frac{\pi k^2}{2} J'_m(k\rho) J'_m(k\rho)\cos(m(\theta-\phi)) \quad (26)$$

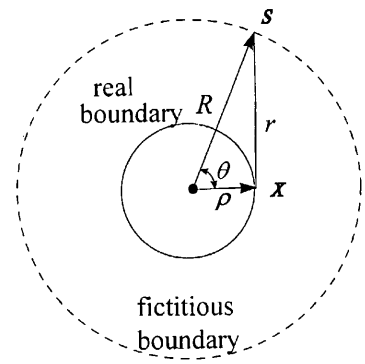

(a)

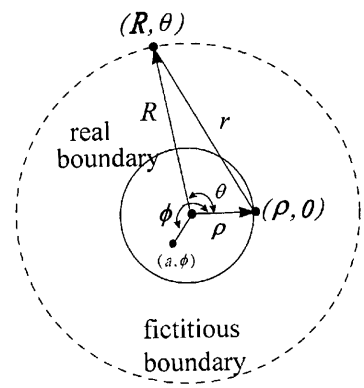

(b)

Fig. 1. (a) The definitions of ρ, θ, and R. (b) The definitions of ρ, θ, ϕ, a and R.

after substituting ρ for R in Eqs. (19)~(22). By superimposing $2N$ constant source distribution, u or t, along the real boundary with radius ρ and collocating the $2N$ points on the real boundary with radius ρ for the direct method, we have

$$[U] = [U^i] = [U^e]$$

$$= \begin{bmatrix} a_0 & a_1 & a_2 & \cdots & a_{2N-2} & a_{2N-1} \\ a_{2N-1} & a_0 & a_1 & \cdots & a_{2N-3} & a_{2N-2} \\ a_{2N-2} & a_{2N-1} & a_0 & \cdots & a_{2N-4} & a_{2N-3} \\ \vdots & \vdots & \vdots & \ddots & \vdots & \vdots \\ a_1 & a_2 & a_3 & \cdots & a_{2N-1} & a_0 \end{bmatrix} \quad (27)$$

$$[T] = [T^i] = [T^e]$$

$$= \begin{bmatrix} b_0 & b_1 & b_2 & \cdots & b_{2N-2} & b_{2N-1} \\ b_{2N-1} & b_0 & b_1 & \cdots & b_{2N-3} & b_{2N-2} \\ b_{2N-2} & b_{2N-1} & b_0 & \cdots & b_{2N-4} & b_{2N-3} \\ \vdots & \vdots & \vdots & \ddots & \vdots & \vdots \\ b_1 & b_2 & b_3 & \cdots & b_{2N-1} & b_0 \end{bmatrix} \quad (28)$$

$$[L]=[L^i]=[L^e]$$

$$=\begin{bmatrix} c_0 & c_1 & c_2 & \cdots & c_{2N-2} & c_{2N-1} \\ c_{2N-1} & c_0 & c_1 & \cdots & c_{2N-3} & c_{2N-2} \\ c_{2N-2} & c_{2N-1} & c_0 & \cdots & c_{2N-4} & c_{2N-3} \\ \vdots & \vdots & \vdots & \ddots & \vdots & \vdots \\ c_1 & c_2 & c_3 & \cdots & c_{2N-1} & c_0 \end{bmatrix} \tag{29}$$

$$[M]=[M^i]=[M^e]$$

$$=\begin{bmatrix} d_0 & d_1 & d_2 & \cdots & d_{2N-2} & d_{2N-1} \\ d_{2N-1} & d_0 & d_1 & \cdots & d_{2N-3} & d_{2N-2} \\ d_{2N-2} & d_{2N-1} & d_0 & \cdots & d_{2N-4} & d_{2N-3} \\ \vdots & \vdots & \vdots & \ddots & \vdots & \vdots \\ d_1 & d_2 & d_3 & \cdots & d_{2N-1} & d_0 \end{bmatrix} \tag{30}$$

where the superscripts "i" and "e" denote the interior and exterior domains, respectively, and $[U]$, $[T]$, $[L]$ and $[M]$ are the influence matrices with the elements shown below:

$$a_m=\int_{(m-\frac{1}{2})\Delta\theta}^{(m+\frac{1}{2})\Delta\theta} U(\theta,0)\rho d\theta \approx U(\theta_m,0)\rho\Delta\theta,$$

$$m=0,\ 1,\ 2,\ \ldots,\ 2N-1, \tag{31}$$

$$b_m=\int_{(m-\frac{1}{2})\Delta\theta}^{(m+\frac{1}{2})\Delta\theta} T(\theta,0)\rho d\theta \approx T(\theta_m,0)\rho\Delta\theta,$$

$$m=0,\ 1,\ 2,\ \ldots,\ 2N-1, \tag{32}$$

$$c_m=\int_{(m-\frac{1}{2})\Delta\theta}^{(m+\frac{1}{2})\Delta\theta} L(\theta,0)\rho d\theta \approx L(\theta_m,0)\rho\Delta\theta,$$

$$m=0,\ 1,\ 2,\ \ldots,\ 2N-1, \tag{33}$$

$$d_m=\int_{(m-\frac{1}{2})\Delta\theta}^{(m+\frac{1}{2})\Delta\theta} M(\theta,0)\rho d\theta \approx M(\theta_m,0)\rho\Delta\theta,$$

$$m=0,\ 1,\ 2,\ \ldots,\ 2N-1, \tag{34}$$

where $\Delta\theta=\frac{2\pi}{2N}$ and $\theta_m=m\Delta\theta$. The matrices, $[U]$, $[T]$, $[L]$ and $[M]$, are found to be in circulant forms since rotation symmetry for the influence coefficients exists. By introducing the following bases for the circulants (Golberg, 1991): I, C_{2N}^1, C_{2N}^2, ..., C_{2N}^{2N-1}, we can expand the four matrices into

$$[U]=a_0I+a_1C_{2N}^1+a_2C_{2N}^2+\cdots+a_{2N-1}C_{2N}^{2N-1}, \tag{35}$$

$$[T]=b_0I+b_1C_{2N}^1+b_2C_{2N}^2+\cdots+b_{2N-1}C_{2N}^{2N-1}, \tag{36}$$

$$[L]=c_0I+c_1C_{2N}^1+c_2C_{2N}^2+\cdots+c_{2N-1}C_{2N}^{2N-1}, \tag{37}$$

$$[M]=d_0I+d_1C_{2N}^1+d_2C_{2N}^2+\cdots+d_{2N-1}C_{2N}^{2N-1}, \tag{38}$$

where $[I]$ is a unit matrix and

$$C_{2N}=\begin{bmatrix} 0 & 1 & 0 & \cdots & 0 & 0 \\ 0 & 0 & 1 & \cdots & 0 & 0 \\ \vdots & \vdots & \vdots & \ddots & \vdots & \vdots \\ 0 & 0 & 0 & \cdots & 0 & 1 \\ 1 & 0 & 0 & \cdots & 0 & 0 \end{bmatrix}_{2N\times 2N}. \tag{39}$$

Based on the similar properties of the matrices of $[U]$, $[T]$, $[L]$, $[M]$ and $[C_{2N}]$, the eigenvalues can be derived as shown below:

$$\lambda_\ell=a_0+a_1\alpha_\ell+a_2\alpha_\ell^2+\cdots+a_{2N-1}\alpha_\ell^{2N-1},$$

$$\ell=0,\ \pm1,\ \pm2,\ \ldots,\ \pm(N-1),\ N, \tag{40}$$

$$\mu_\ell=b_0+b_1\alpha_\ell+b_2\alpha_\ell^2+\cdots+b_{2N-1}\alpha_\ell^{2N-1},$$

$$\ell=0,\ \pm1,\ \pm2,\ \ldots,\ \pm(N-1),\ N, \tag{41}$$

$$\nu_\ell=c_0+c_1\alpha_\ell+c_2\alpha_\ell^2+\cdots+c_{2N-1}\alpha_\ell^{2N-1},$$

$$\ell=0,\ \pm1,\ \pm2,\ \ldots,\ \pm(N-1),\ N, \tag{42}$$

$$\delta_\ell=d_0+d_1\alpha_\ell+d_2\alpha_\ell^2+\cdots+d_{2N-1}\alpha_\ell^{2N-1},$$

$$\ell=0,\ \pm1,\ \pm2,\ \ldots,\ \pm(N-1),\ N, \tag{43}$$

where λ_ℓ, μ_ℓ, ν_ℓ and δ_ℓ are eigenvalues for $[U]$, $[T]$, $[L]$ and $[M]$, respectively, and α_ℓ are the eigenvalues for the matrix $[C_{2N}]$. It is easily found that the eigenvalues, α_n, and eigenvectors, $\{\phi\}_n$, for the circulants $[C_{2N}]$ are the roots for $\alpha^{2N}=1$ as shown below:

$$\alpha_n=e^{i\frac{2\pi n}{2N}},\ n=0,\ \pm1,\ \pm2,\ \ldots,\ \pm(N-1),\ N$$

$$\text{or } n=0,\ 1,\ 2,\ \ldots,\ 2N-1, \tag{44}$$

$$\{\phi\}_n=\begin{Bmatrix} 1 \\ \alpha_n \\ \alpha_n^2 \\ \alpha_n^3 \\ \vdots \\ \alpha_n^{2N-1} \end{Bmatrix},\ n=0,\ \pm1,\ \pm2,\ \ldots,\ \pm(N-1),\ N$$

$$\text{or } n=0,\ 1,\ 2,\ \ldots,\ 2N-1, \tag{45}$$

respectively.

Substituting Eq. (44) into Eq. (40), we have

$$\lambda_\ell = \sum_{m=0}^{2N-1} a_m \alpha_\ell^m = \sum_{m=0}^{2N-1} a_m e^{i\frac{2\pi}{2N}m\ell},$$

$$\ell = 0, \pm 1, \pm 2, \ldots, \pm(N-1), N. \quad (46)$$

According to the definition for a_m in Eq. (31), we have

$$a_m = a_{2N-m},\ m = 0, 1, 2, \ldots, 2N-1. \quad (47)$$

Substituting Eq. (47) into Eq. (46), we have

$$\lambda_\ell = a_0 + (-1)^\ell a_N + \sum_{m=1}^{N-1} (\alpha_\ell^m + \alpha_\ell^{2N-m}) a_m$$

$$= \sum_{m=0}^{2N-1} \cos(m\ell\Delta\theta) a_m . \quad (48)$$

Substituting a_m in Eq. (31) into Eq. (48), we have

$$\lambda_\ell \approx \sum_{m=0}^{2N-1} \cos(m\ell\Delta\theta) U(m\ell\Delta\theta, 0)\rho\Delta\theta$$

$$= \int_0^{2\pi} \cos(\ell\theta) U(\theta, 0)\rho d\theta \quad (49)$$

as N approaches infinity. Eq. (49) reduces to

$$\lambda_\ell = \int_0^{2\pi} \cos(\ell\theta) \sum_{m=-\infty}^{\infty} \frac{-\pi}{2} J_m(k\rho) J_m(k\rho) \cos m\theta \rho d\theta$$

$$= -\pi^2 \rho J_\ell(k\rho) J_\ell(k\rho) . \quad (50)$$

Similarly, we have

$$\mu_\ell = -\pi^2 k\rho J'_\ell(k\rho) J_\ell(k\rho) \quad (51)$$

$$\nu_\ell = -\pi^2 k\rho J_\ell(k\rho) J'_\ell(k\rho) \quad (52)$$

$$\delta_\ell = -\pi^2 k^2 \rho J'_\ell(k\rho) J'_\ell(k\rho) \quad (53)$$

where μ_ℓ, ν_ℓ, δ_ℓ are the eigenvalues of $[T]$, $[L]$ and $[M]$ matrices, respectively. Since the wave number k is imbedded in each element of the circulant matrices, the corresponding eigenvalues for the four matrices are also functions of k. Finding the eigenvalues for the Helmholtz eigenproblem or finding the zeros for the determinant of the circulants is equal to finding the zeros for the multiplication of all their eigenvalues. The determinant can be obtained as follows:

$$\det[U] = \lambda_0 \lambda_N (\lambda_1 \lambda_2 \ldots \lambda_{N-1})(\lambda_{-1} \lambda_{-2} \ldots \lambda_{-(N-1)}), \quad (54)$$

$$\det[T] = \mu_0 \mu_N (\mu_1 \mu_2 \ldots \mu_{N-1})(\mu_{-1} \mu_{-2} \ldots \mu_{-(N-1)}), \quad (55)$$

$$\det[L] = \nu_0 \nu_N (\nu_1 \nu_2 \ldots \nu_{N-1})(\nu_{-1} \nu_{-2} \ldots \nu_{-(N-1)}), \quad (56)$$

$$\det[M] = \delta_0 \delta_N (\delta_1 \delta_2 \ldots \delta_{N-1})(\delta_{-1} \delta_{-2} \ldots \delta_{-(N-1)}), \quad (57)$$

Since the alternating properties for the Bessel function can be obtained, *i.e.*,

$$J_{-\ell}(k\rho) = (-1)^\ell J_\ell(k\rho), \quad \ell \in N, \quad (58)$$

$$J'_{-\ell}(k\rho) = (-1)^\ell J'_\ell(k\rho), \quad \ell \in N, \quad (59)$$

Eqs. (54)~(57) can be reduced to

$$\det[U] = \lambda_0 (\lambda_1 \lambda_2 \ldots \lambda_{N-1})^2 \lambda_N . \quad (60)$$

$$\det[T] = \mu_0 (\mu_1 \mu_2 \ldots \mu_{N-1})^2 \mu_N . \quad (61)$$

$$\det[L] = \nu_0 (\nu_1 \nu_2 \ldots \nu_{N-1})^2 \nu_N . \quad (62)$$

$$\det[M] = \delta_0 (\delta_1 \delta_2 \ldots \delta_{N-1})^2 \delta_N . \quad (63)$$

The square terms in Eqs. (60)~(63) imply that double roots occur for λ_ℓ when $\ell = 1, 2, \ldots, N-1$. In order to verify that either $J_\ell(k\rho)=0$ or $J'_\ell(k\rho)=0$ is a true eigenequation, the dual formulation is needed to distinguish the true and spurious solutions.

The possible (true or spurious) eigenvalues occur at

$$J_\ell(k\rho) J_\ell(k\rho) = 0, \quad \ell = 0, \pm 1, \pm 2, \ldots, \pm(N-1), N. \quad (64)$$

for the Dirichlet problem using the UT method since the determinant of $[U]$ matrix is zero.

For the LM method, the possible (true or spurious) eigenvalues occur at

$$J_\ell(k\rho) J'_\ell(k\rho) = 0, \quad \ell = 0, \pm 1, \pm 2, \ldots, \pm(N-1), N. \quad (65)$$

for the Dirichlet problem since the determinant of $[L]$ matrix is zero.

After comparing the results from the dual formulation in Eqs. (64) and (65), we can determine the true and spurious eigenequation for the Dirichlet problem as follows:

True eigenequation:

$$J_\ell(k\rho) = 0, \quad \ell = 0, \pm 1, \pm 2, \ldots, \pm(N-1), N. \quad (66)$$

Spurious eigenequation:

$$J'_\ell(k\rho) = 0, \quad \ell = 0, \pm 1, \pm 2, \ldots, \pm(N-1), N. \quad (67)$$

Similarly, we can extend the Dirichlet problem to the Neumann problem.

After comparing the results obtained by the dual formulation, we can summarize the spurious eigenequations for both the Dirichlet and Neumann

Table 3. The true and spurious eigenequations for a two-dimensional circular cavity under Dirichlet and Neumann boundary conditions using the dual formulations.

	Interior Dirichlet problem		Interior Neumann problem	
Kernels	True eigenequation	Spurious eigenequation	True eigenequation	Spurious eigenequation
U_C, T_C	$J_n(ka)=0$	×	$J_n'(ka)=0$	×
L_C, M_C	$J_n(ka)=0$	×	$J_n'(ka)=0$	×
U_R, T_R	$J_n(ka)=0$	$Y_n(ka)=0$	$J_n'(ka)=0$	$Y_n(ka)=0$
L_R, M_R	$J_n(ka)=0$	$Y_n'(ka)=0$	$J_n'(ka)=0$	$Y_n'(ka)=0$
U_I, T_I	$J_n(ka)=0$	$J_n(ka)=0$	$J_n'(ka)=0$	$J_n(ka)=0$
L_I, M_I	$J_n(ka)=0$	$J_n'(ka)=0$	$J_n'(ka)=0$	$J_n'(ka)=0$

where n=0, 1, 2, 3, ...

Table 4. The true and spurious eigenequations for a one-dimensional rod under Dirichlet and Neumann boundary conditions using the dual formulations.

	Interior Dirichlet problem ($u(0)=0$, $u(1)=0$)		Interior Neumann problem ($t(0)=0$, $t(1)=0$)	
Kernels	True eigenequation	Spurious eigenequation	True eigenequation	Spurious eigenequation
U_C, T_C	$\sin\sqrt{\lambda}=0$	×	$\sin\sqrt{\lambda}=0$	×
L_C, M_C	$\sin\sqrt{\lambda}=0$	×	$\sin\sqrt{\lambda}=0$	×
U_R, T_R	$\sin\sqrt{\lambda}=0$	$\sin\sqrt{\lambda}=0$	$\sin\sqrt{\lambda}=0$	$\sin\sqrt{\lambda}=0$
L_R, M_R	$\sin\sqrt{\lambda}=0$	$\sin\sqrt{\lambda}=0$	$\sin\sqrt{\lambda}=0$	$\sin\sqrt{\lambda}=0$
U_I, T_I	$\sin\sqrt{\lambda}=0$	$\sin\sqrt{\lambda}=0$	$\sin\sqrt{\lambda}=0$	$\sin\sqrt{\lambda}=0$
L_I, M_I	$\sin\sqrt{\lambda}=0$	$\sin\sqrt{\lambda}=0$	$\sin\sqrt{\lambda}=0$	$\sin\sqrt{\lambda}=0$
	Interior mixed problem ($u(0)=0$, $u(1)=0$)		Interior mixed problem ($u(1)=0$, $t(0)=0$)	
Kernels	True eigenequation	Spurious eigenequation	True eigenequation	Spurious eigenequation
U_C, T_C	$\cos\sqrt{\lambda}=0$	×	$\cos\sqrt{\lambda}=0$	×
L_C, M_C	$\cos\sqrt{\lambda}=0$	×	$\cos\sqrt{\lambda}=0$	×
U_R, T_R	$\cos\sqrt{\lambda}=0$	$\sin\sqrt{\lambda}=0$	$\cos\sqrt{\lambda}=0$	$\sin\sqrt{\lambda}=0$
L_R, M_R	$\cos\sqrt{\lambda}=0$	$\sin\sqrt{\lambda}=0$	$\cos\sqrt{\lambda}=0$	$\sin\sqrt{\lambda}=0$
U_I, T_I	$\cos\sqrt{\lambda}=0$	$\sin\sqrt{\lambda}=0$	$\cos\sqrt{\lambda}=0$	$\sin\sqrt{\lambda}=0$
L_I, M_I	$\cos\sqrt{\lambda}=0$	$\sin\sqrt{\lambda}=0$	$\cos\sqrt{\lambda}=0$	$\sin\sqrt{\lambda}=0$

where $\lambda=k^2$, $U_R(s,x)=\dfrac{\sin(kr)}{2k}$ and $U_I(s,x)=\dfrac{-\cos(kr)}{2k}$.

problems:

$$J_\ell(k\rho)=0 \text{ using the } UT \text{ quation,} \tag{68}$$

$$J_\ell'(k\rho)=0 \text{ using the } LM \text{ equation,} \tag{69}$$

The true eigenequations using the *UT* or *LM* method are found to be:

$$J_\ell(k\rho)=0 \text{ for the Dirichlet problem,} \tag{70}$$

$$J_\ell'(k\rho)=0 \text{ for the Neumann problem.} \tag{71}$$

The above results are summaized in Table 3. The true and spurious solutions using real-part kernels are also included in the table for comparison. For the special case of the one-dimensional rod problem, the true and spurious solutions subjected to different boundary conditions using the real and imaginary-part kernels are shown in Table 4. Table 3 indicates that spurious solution depends on the chosen method, the *UT* or *LM* formulation, and true solution depends on the types of the boundary conditions, the Dirichlet or Neumann problem. After determining the eigenvalues, the boundary modes are our concern. It is interesting to find that both the true and spurious boundary modes are found to be the same as shown in Eq. (45) since the matrices are both similar to the circulant in Eq. (39). That is to say, looking at the boundary modes may mislead the judgement for true and spurious solutions. For example, Fig. 2 shows that the true and spurious boundary modes are the same. Fig. 3 shows that the nodal lines for the true and spurious interior modes look similar. However, the spurious eigenvalues for the Dirichlet problem using the *UT* method are the same as true eigenvalues. This means that the true multiplicity is changed to spurious multiplicity of double value. For the case

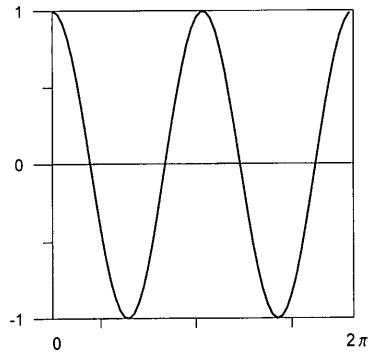

(a) True boundary mode $t(\theta)=\cos 2\theta$ for the Dirichlet problem.

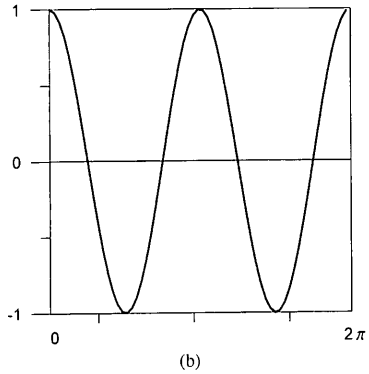

(b)

(b) Spurious boundary mode $t(\theta)=\cos 2\theta$ for the Dirichlet problem.

Fig. 2. The true and spurious boundary modes.

of $\ell=0$, true multiplicity of one will be changed to two of spurious multiplicity. For the case of $\ell\neq 0$, true multiplicity of two will be changed to four of spurious multiplicity. In the same way, we can extend the results to a Neumann problem when the *LM* method is used.

V. ANALYTICAL DERIVATIONS FOR TRUE AND SPURIOUS INTERIOR MODE

After we obtain the eigenvalues, boundary modes for the Dirichlet problem, we can derive the interior mode by using the real-part formulation (Chen *et. al.*, 1999b) as shown below:

$$u_n(a,\phi)=-\sum_{\ell=0}^{2N-1} U_a(\ell\Delta\theta-\phi,0)\,\overline{t}_{\ell n}\rho\Delta\theta$$

$$=-\sum_{\ell=0}^{2N-1} U_a(\ell\Delta\theta-\phi,0)\cos(\ell n\Delta\theta)\rho\Delta\theta$$

$$=-\int_0^{2\pi} U_a(\theta-\phi,0)\cos(n\theta)\rho d\theta$$

$$=-\int_0^{2\pi}\sum_{m=-\infty}^{\infty}\frac{\pi}{2}J_m(ka)Y_m(k\rho)\cos(m(\theta-\phi))\cos(n\theta)\rho d\theta$$

$$=-\pi^2\rho J_n(ka)Y_n(k\rho)\cos(n\phi),\quad 0<a<\rho,\ 0<\phi<2\pi \qquad (72)$$

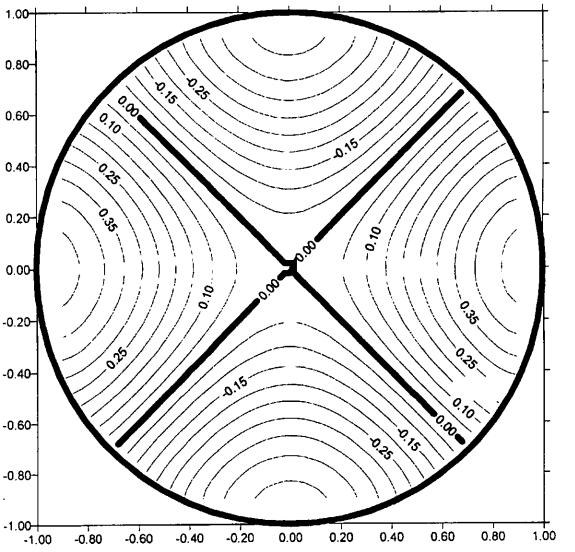

(a)

(a) Spurious interior mode $u_2(a,\phi)=J_1(3.0542a)\cos 2\phi$

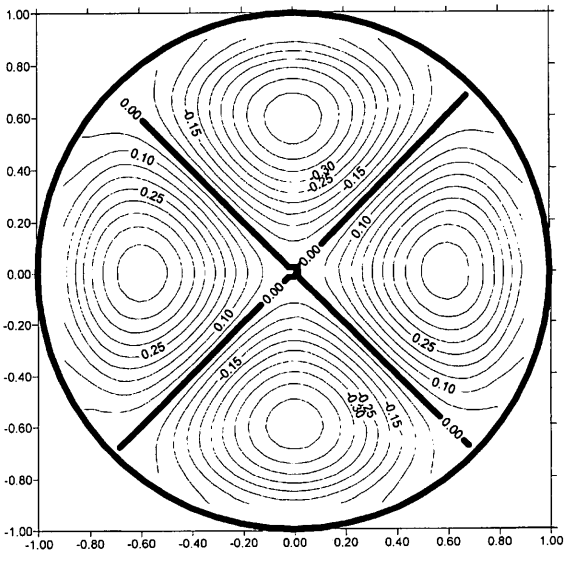

(b)

(b) True interior mode $u_2(a,\phi)=J_2(5.1356a)\cos 2\phi$

Fig. 3. The true and spurious interior modes.

where the real part for the ℓ th component, $\overline{t}_{\ell n}$ in the eigenvector $\{\phi\}_n$ of Eq. (45) is adopted. If the sine part of the eigenvector in Eq. (45) is chosen, the interior mode becomes

$$u_n(a,\phi)=-\pi^2\rho J_n(ka)Y_n(k\rho)\sin(n\phi),$$

$$0<a<\rho,\ 0<\phi<2\pi. \qquad (73)$$

Eq. (72) shows the interior modes when k represents the true eigenvalues for the Dirichlet problems which satisfy $J_n(k\rho)=0$ as shown in Eq. (66). Also,

Table 5. The true and spurious systems for the Dirichlet problem (u=0) using the imaginary-part *UT* and *LM* BEMs.

	Eigenequation		Eigenmode (boundary)	Eigenmode (interior): $u_n(a,\phi)$ (unnormalized) Eigenmode (interior): $\overline{u}_n(a,\phi)$ (normalized)
UT method	True	$J_n(k\rho)=0$	$e^{in\theta}$	$u_n(a,\phi)=-\pi^2\rho J_n(ka)Y_n(k\rho)\cos(n\phi)$* $\overline{u}_n(a,\phi)=J_n(ka)\cos(n\phi)$**
	Spurious	$J_n(k\rho)=0$	$e^{in\theta}$	$u_n(a,\phi)=-\pi^2\rho J_n(ka)Y_n(k\rho)\cos(n\phi)$*** $\overline{u}_n(a,\phi)=J_n(ka)\cos(n\phi)$**
LM method	True	$J_n(k\rho)=0$	$e^{in\theta}$	$u_n(a,\phi)=-\pi^2\rho J_n(ka)Y_n(k\rho)\cos(n\phi)$* $\overline{u}_n(a,\phi)=J_n(ka)\cos(n\phi)$**
	Spurious	$J_n'(k\rho)=0$	$e^{in\theta}$	$u_n(a,\phi)=-\pi^2\rho J_n(ka)Y_n(k\rho)\cos(n\phi)$*** $\overline{u}_n(a,\phi)=J_n(ka)\cos(n\phi)$**

"*" denotes the notrivial solution, "**" denotes the nontrivial solution after normalization and "***" denotes the trivial solution without normalization

Eq. (72) shows the spurious modes when k represents the spurious eigenvalues which satisfy $J_n(k\rho)=0$ as shown in Eq. (68). However, the true mode can be normalized as

$$\overline{u}_n(a,\phi)=\frac{u_n(a,\phi)}{-\pi^2\rho Y_n(k\rho)}=J_n(ka)\cos(n\phi), \tag{74}$$

where $\overline{u}_n(a,\phi)$ is a normalized mode,

If the *LM* method for the Dirichlet problem is applied, the interior mode is

$$u_n(a,\phi)=-\pi^2\rho J_n(ka)Y_n(k\rho)\cos(n\phi),$$

$$0<a<\rho,\ 0<\phi<2\pi. \tag{75}$$

It is found that the modal shapes are the same using *UT* and *LM* methods after comparing Eqs. (72) and (75). However, their spurious eigenequations are not the same as shown in Eqs. (64) and (65). The spurious modes are obtained by substituting the spurious eigenvalues ($J_n'(k\rho)=0$) into Eq. (75), while the true modes are obtained by substituting the true eigenvalues ($J_n(k\rho)=0$) into Eq. (75). After normalization with respect to $Y_n(k\rho)$, the true and spurious modes are shown in Fig. 3 for n=2. Fig. 3 indicates that the nodal lines for the true and spurious modes are the same. Nevertheless, the true and spurious modes are quite different since the values of k are not the same (one is true and the other is spurious). This finding warns us that Hutchinson's sorting technique by looking at the modal shapes may mislead us to make a wrong judgement for true and spurious solutions.

For the Neumann problem, we have

$$u_n(a,\phi)=\int_0^{2\pi}\sum_{m=-\infty}^{\infty}\frac{k\pi}{2}J_m(ka)Y_m'(k\rho)\cos(m(\theta-\phi))\cos(n\theta)\rho d\theta$$

$$=\pi^2 k\rho J_n(ka)Y_n'(k\rho)\cos(n\phi),\ 0<a<\rho,\ 0<\phi<2\pi, \tag{76}$$

using the direct *UT* method. Eq. (76) shows the interior modes when k is true eigenvalue for the Neumann problems which satisfies $J_n'(k\rho)=0$. Eq.(76) shows the spurious modes when k represents spurious eigenvalues which satisfy $J_n(k\rho)=0$. However, the true modes can be normalized as

$$\overline{u}_n(a,\phi)=\frac{u_n(a,\phi)}{\pi^2 k\rho Y_n'(k\rho)}=J_n(ka)\cos(n\phi), \tag{77}$$

where $\overline{u}_n(a,\phi)$ is a normalized mode. In the same way, the nodal lines for true and spurious modes are found to be the same. Also, their modes (true or spurious) are not exactly the same. Hutchinson's sorting technique by examining the modal shapes may fail to separate the true and spurious solutions.

If the *LM* method is employed to solve the Neumann problem, we have

$$\overline{u}_n(a,\phi)=\pi^2 k\rho J_n(ka)Y_n'(k\rho)\cos(n\phi),$$

$$0<a<\rho,\ 0<\phi<2\pi. \tag{78}$$

It is found that the modal shapes are the same using the *UT* and *LM* methods. Since the true and spurious eigenequations are the same to $J_n'(k\rho)=0$ as shown in Eqs. (69) and (71), this also results in spurious multiplicity. However, the normalized modes are

$$\overline{u}_n(a,\phi)=\frac{u_n(a,\phi)}{\pi^2\rho Y_n'(k\rho)}=J_n(ka)\cos(n\phi) \tag{79}$$

where $\overline{u}_n(a,\phi)$ is a normalized mode. The eigenequation, boundary modes and interior modes for the Dirichlet and Neumann problems using the direct *UT* or *LM* methods are summarized in Tables 5 and 6, respectively. Both the normalized and unnormalized solutions are included.

Table 6. The true and spurious systems for the Neumann problem (t=0) using the imaginary-part *UT* and *LM* BEMs.

	Eigenequation		Eigenmode (boundary)	Eigenmode (interior): $u_n(a,\phi)$ (unnormalized) Eigenmode (interior): $\overline{u}_n(a,\phi)$ (normalized)
UT	True	$J_n'(k\rho)=0$	$e^{in\theta}$	$u_n(a,\phi)=\pi^2 k\rho J_n(ka)Y_n'(k\rho)\cos(n\phi)$* $\overline{u}_n(a,\phi)=J_n(ka)\cos(n\phi)$**
method	Spurious	$J_n(k\rho)=0$	$e^{in\theta}$	$u_n(a,\phi)=\pi^2 k\rho J_n(ka)Y_n'(k\rho)\cos(n\phi)$* $\overline{u}_n(a,\phi)=J_n(ka)\cos(n\phi)$*
LM	True	$J_n'(k\rho)=0$	$e^{in\theta}$	$u_n(a,\phi)=\pi^2 k\rho J_n(ka)Y_n'(k\rho)\cos(n\phi)$* $\overline{u}_n(a,\phi)=J_n(ka)\cos(n\phi)$**
method	Spurious	$J_n'(k\rho)=0$	$e^{in\theta}$	$u_n(a,\phi)=\pi^2 k\rho J_n(ka)Y_n'(k\rho)\cos(n\phi)$*** $\overline{u}_n(a,\phi)=J_n(ka)\cos(n\phi)$**

"*" denotes the notrivial solution, "**" denotes the nontrivial solution after normalization and "***" denotes the trivial solution without normalization

VI. CONCLUDING REMARKS

In this paper, a nonsingular integral formulation for the Helmholtz eigenproblem was proposed using only imaginary-part kernels instead of complex kernels. Since there is no source in the auxilliary system, only regular integrals are encountered. An analytical example for a circular domain is studied by using the dual series model. Based on the analytical properties of the circulants, the true and spurious eigensolutions can be distinguished after comparing the eigenequations obtained from the dual formulation. Also, the possible failure of Hutchinson's sorting technique for spurious solutions is discussed and the spurious multiplicity is examined. These results provide the basis for comparison with further numerical studies.

ACKNOWLEDGEMENTS

Financial support from the National Science Council, under Grant No. NSC 89-2211-E-019-003 is gratefully acknowledged.

REFERENCES

1. Chen, J.T., 1998, "On Fictitious Frequencies Using Dual Series Representation," *Mechanics Research Communications*, Vol. 25, pp. 529-534.
2. Chen, J.T., 1999, "Recent Development of Dual BEM in Acoustic Problems," *Computer Methods in Applied Mechanics and Engineering*, Accepted.
3. Chen, J.T., and Chen, K.H., 1998, "Dual Integral Formulation for Determining the Acoustic Modes of a Two-dimensional Cavity with a Degenerate Boundary", *Engineering Analysis with Boundary Elements*, Vol. 21, pp. 105-116.
4. Chen, J.T., Chen, K.H., and Chyuan, S.W., 1999a, "Numerical Experiments for Acoustic Modes of a Square Cavity using Dual BEM," *Appl. Acoust.*, Vol. 57, pp. 293-325.
5. Chen, J.T., and Hong, H.-K., 1992, *Boundary element method*, New World Press 2nd Ed., Taipei, Taiwan (in Chinese).
6. Chen, J.T., and Hong, H.-K., 1999, "Review of Dual Integral Representations with Emphasis on Hypersingular Integrals and Divergent Series", *Transactions of ASME, Applied Mechanics Reviews*, Vol. 52, pp. 17-33.
7. Chen, J.T., Huang, C.X., and Chen, K.H., 1999b, "Determination of Spurious Eigenvalues and Multiplicities of True Eigenvalues Using the Real-part Dual BEM," *Computational Mechanics*, Vol. 24, pp. 41-51.
8. Chen, J.T., Huang, C.X., and Wong, F.C., 1999b, "Determination of Spurious Eigenvalues and Multiplicities of True Eigenvalues in the Dual Multiple Reciprocity Method Using the Singular Value Decomposition Technique," *Journal of Sound and Vibration*, Accepted.
9. Chen, J.T., Huang, C.S., and Wong, F.C., 1998, "Analysis and Experiment for Acoustic Modes of a Cavity Containing an Incomplete Partition," *Proceedings of the Fourth National Conference on Structural Engineering*, Vol. 1, pp. 349-356.
10. Chen, J.T., Liang, M.T., Chen, I.L., Chyuan, S. W., and Chen, K. H., 1999c, "Dual Boundary Element Analysis of Wave Scattering from Singularities," *Wave Motion*, Vol. 30, pp. 367-381.
11. Chen, J.T., and Wong, F.C., 1997, "Analytical Derivations for One-dimensional Eigenproblems Using Dual BEM and MRM," *Engineering Analysis with Boundary Elements*, Vol. 20, pp.25-33.
12. Chen, J.T., and Wong, F.C., 1998, "Dual Formulation of Multiple Reciprocity Method for the Acoustic Mode of a Cavity with a Thin Partition," *Journal of Sound and Vib*ration, Vol. 217, pp. 75-95.

13. Chen, K.H., Chen, J.T., and Liou, D.Y., 1998, "Dual Boundary Element Analysis for an Acoustic Cavity with an Incomplete Partition," *Chinese J. Mech.*, Vol. 14, pp. 1-14 (in Chinese).
14. De Mey, G., 1976, "Calculation of the Helmholtz Equation by an Integral Equation," *International Journal Numerical Methods in Engineering*, Vol. 10, pp. 59-66.
15. De Mey, G., 1977, "A Simplified Integral Equation Method for the Calculation of the Eigenvalues of Helmholtz Equation," *International Journal Numerical Methods in Engineering*, Vol. 11, pp. 1340-1342.
16. Goldberg J.L., 1991, *Matrix Theory with Applications*, McGraw-Hill, New York.
17. Hutchinson, J. R., 1988, "Vibration of Plates", in *Boundary Elements X*, Vol.4, Brebbia C. A. (ed), Springer-Verlag, Berlin, pp. 415-430.
18. Hutchinson, J.R., 1985, "An Alternative BEM Formulation Applied to Membrane Vibrations", in *Boundary Elements VII*, C. A. Brebbia and G. Maier Eds., Springer-Verlag.
19. Hutchinson, J.R., 1991, "Analysis of Plates and Shells by Boundary Collocation," in *Boundary Element Analysis of Plates and Shells*, Beskos D. E. (ed), Springer-Verlag, Berlin, pp. 314-368.
20. Kamiya, N., Andoh, E., and Nogae, K., 1996, "A New Complex-valued Formulation and Eigenvalue Analysis of the Helmholtz Equation by Boundary Element Method," *Advances in Engineering Software*, Vol. 26, pp. 219-227.
21. Liou, D.Y., Chen, J.T., and Chen, K.H., 1999, "A New Method for Determining the Acoustic Modes of a Two-dimensional Sound Field," *Journal of Chinese Institute of Civil and Hydraulic Engineering*, Vol.11, No.2, pp.89-100 (in Chinese).
22. Nowak, A.J., and Neves, A.C. eds., 1994, *Multiple Reciprocity Boundary Element Method*, Southampton: Competational Mechunics Publications.
23. Tai, G R.G., and Shaw, R.P., 1974, "Helmholtz Equation Eigenvalues and Eigenmodes for Arbitrary Domains," *Journal of Acoustical Society of America*, Vol. 56, pp. 796-804.
24. Yeih, W., Chen, J.T., Chen, K.H., and Wong, F.C., 1997, "A Study on the Multiple Reciprocity Method and Complex-valued Formulation for the Helmholtz Equation," *Advances in Engineering Software*, Vol. 29, pp. 1-6.
25. Yeih, W., Chang, J.R., Chang, C.M,. and Chen, J.T., 1999, "Applications of Dual MRM for Determining the Natural Frequencies and Natural Modes of a Rod Using the Singular Value Decomposition Method," *Advances in Engineering Software*, Vol.30, No. 7, pp. 459-468.
26. Yeih, W., Chen, J.T., and Chang, C.M., 1999, "Applications of Dual MRM for Determining the Natural Frequencies and Natural Modes of an Euler-Bernoulli Beam Using the Singular Value Decomposition Method," *Engineering Analysis with Boundary Elements*, Vol. 23, pp. 339-360.

Discussions of this paper may appear in the discussion section of a future issue. All discussions should be submitted to the Editor-in-Chief.

Manuscript Received: June 06, 1999
Revision Received: July 20, 1999
and Accepted: Aug. 07, 1999

Helmholtz 特徵值問題非奇異積分推導

陳正宗　郭世榮　陳桂鴻

國立台灣海洋大學河海工程學系

摘　要

本文針對 Helmholtz 特徵值問題發展一非奇異積分推導解法。此法僅採用複數核函數中的虛部。基於此不含奇異源的輔助系統，奇異與超奇異積分將不會出現。然而，卻會導致假的特徵解。配合對偶架構後，眞假特徵解可被分辨出來。利用循環對稱矩陣可解析的特性，一個圓形範例，將可解析推導並說明眞假特徵解的發生機制。同時，包括眞假特徵值、眞假特徵邊界狀態、眞假內域模態與眞假重根數均有所探討。另Hutchinson由模態鑑別眞假解的技巧可行性，在本文亦加以討論。

關鍵詞：虛部對偶邊界元素法；假特徵根與假模態，Bessel 函數與 Helmholtz 方程。